

PACS numbers: 42.65.Re; 42.60.By; 42.79.Dj
DOI: 10.1070/QE2012v042n11ABEH014966

Alignment of chirped-pulse compressor

I.V. Yakovlev

Abstract. **An original method of alignment of grating compressors for ultrahigh-power CPA laser systems is proposed. The use of this method for adjustment of the grating compressor of a PEARL subpetawatt laser complex made it possible to align the diffraction gratings with a second accuracy in all three angular degrees of freedom, including alignment of the grooves, and to adjust the angles of beam incidence on the grating with a high accuracy. A simple method for measuring the difference in the groove densities of gratings with accuracy better than 0.005 lines mm^{-1} is proposed and tested.**

Keywords: *chirped-pulse amplification, petawatt lasers, stretcher, compressor, angular dispersion, tiled gratings.*

1. Introduction

Among the main devices for chirped pulse amplification (CPA) are pulse stretchers and compressors [1]. Most widely used stretchers and compressors are based on diffraction gratings [2, 3], because gratings have record-high dispersion and can ensure the maximum stretching (compression) coefficients. The characteristics of recompressed pulses at the exit of a CPA system (duration, contrast, presence of satellites) depend on the matching of the stretcher and compressor in different orders of phase dispersion. For each of these devices, it is important to position diffraction gratings with a high accuracy so that these gratings with their working surfaces facing each other and separated by a large distance were parallel, as well as to ensure parallelism of their grooves. In addition, the beam incident on the gratings must be directed perpendicular to the grooves at a definite angle to the grating normal. Inaccurate alignment of the mutual positions of the gratings leads to spatial and temporal distortions of femtosecond pulses [4–10]. The residual uncompensated angular dispersion is accompanied by a tilt of the pulse front, which, in turn, decreases the radiation intensity in the focus.

The requirements to the accuracy of alignment of grating compressors are more rigorous for beams with larger cross sections and for pulses with shorter durations. In [11], it was noted that the deviation from the calculated angle of the beam incidence on the grating of the compressor of a Vulcan (Great Britain) CPA laser system by fractions of a degree or from the parallelism of gratings by about ten angular seconds leads to a 1.5-fold increase in the duration of pulses with $\tau = 500$ fs. An increase in the duration of focused radiation with a tilted pulse front was demonstrated in [7], where a 20″ deviation from the parallelism of the compressor gratings for a beam 25 cm in diameter caused an increase in the duration of pulses with $\tau = 30$ fs in the focus by a factor of five.

The adjustment and precise alignment of compressor gratings can be performed using different methods of controlling the scheme and output radiation parameters. Geometric methods are based on measuring the directions of the main or an auxiliary alignment beam reflected by the compressor gratings [12–14]. For alignment, one usually uses broadband or two-frequency radiation [4, 13, 15]. Focusing these beams after passing through the compressor, one can measure the residual angular dispersion. Interferometers, autocorrelators, and spectrographs are also used for precise adjustment of CPA systems [7, 8, 16–18]. In [19], a stretcher–compressor system was optimised by measuring the power of the signal second-harmonic radiation at the compressor exit. Thus, there exists no universal method of adjustment of compressors of ultrahigh-power CPA systems, especially because each system has its own specifics.

In this work, we present an original method of aligning the compressor of a PEARL subpetawatt laser complex developed at the Institute of Applied Physics, Russian Academy of Sciences [20, 21]. This method is based on the alignment of the working surface and grooves of the grating parallel to its vertical rotation axis with a second accuracy. Using this method, we also adjusted the angles of beam incidence on the compressor gratings with a high accuracy. The difference in the groove density of the diffraction gratings used in a compressor is the source of uncompensated residual angular dispersion [6, 22, 23]. We proposed and tested a simple method allowing one to measure the difference in the groove densities of gratings with an accuracy better than 0.005 lines mm^{-1}. It seems especially helpful and promising to use the proposed methods for alignment of compressors with tiled gratings [24, 25].

2. Compressor of a PEARL subpetawatt laser complex

The scheme and the basic principles of operation of the PEARL subpetawatt complex based on optical parametric chirped-pulse amplification in DKDP nonlinear crystals are described in detail in [20, 21, 26–29]. A specific feature of the complex is the frequency conversion in the first amplification stage, owing to which the stretcher and the compressor stretch and compress radiation with different central wavelengths.

I.V. Yakovlev Institute of Applied Physics, Russian Academy of Sciences, ul. Ul'yanova 46, 603950 Nizhnii Novgorod, Russia; e-mail: ivan@ufp.appl.sci-nnov.ru

Received4 July 2012
Kvantovaya Elektronika **42** (11) 996–1001 (2012)
Translated by M.N. Basieva

An original hybrid prism–grating stretcher [30] and a compressor designed according to the classical Treacy scheme [2] were matched up to the fourth order phase dispersion inclusive.

The two-grating double-pass compressor (Fig. 1) was calculated for compression of chirped signal pulses with the central wavelength of 910 nm amplified to 35 J at the beam diameter of 11 cm. In the compressor, we used gold-coated holographic diffraction gratings with a groove density of 1200 lines mm^{-1}. The working surfaces of the firs (small) and the second (large) gratings were 200×240 and 350×240 mm in size, respectively; the grooves were directed along the 240-mm edge. The reflection efficiency of the gratings for the p-polarised (orthogonal to the grooves) signal was $\sim 90\%$ for a beam incident at the Littrow angle for the first diffraction order.

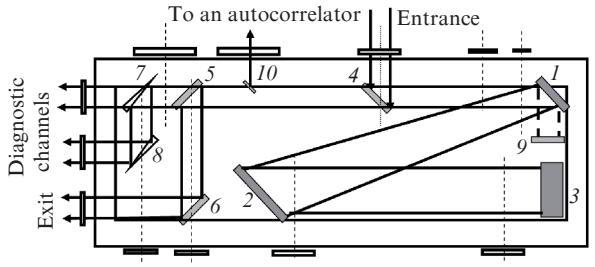

Figure 1. Schematic of a two-grating compressor in a vacuum chamber: (*1*) and (*2*) small and large diffraction gratings, (*3*) vertical roof mirror; (*4*) dichroic input mirror; (*5–8*) output mirrors; (*9*) mirror for zero-order diffraction of the small grating; (*10*) movable mirror.

To eliminate undesired nonlinear self-action effects and retain the beam quality, the compressor was placed in a vacuum chamber designed for a residual pressure of $10^{-5}-10^{-6}$ Torr. The compressor was placed on an optical table supported by vacuum-rubber dampers, which also isolated it from the chamber walls.

The sizes of gratings allowed us to position the beams in two levels. The incident chirped pulse passed through the window of the vacuum chamber and fell onto dichroic mirror (*4*) (reflection coefficient 99.9% for the signal and more than 70% for the He–Ne laser radiation), which, in turn, sent the beam to the small diffraction grating (*1*). Then, the angularly dispersed beam fell on the large grating (*2*), was reflected and recollimated by it, and hit a roof mirror (*3*), which reflected it parallel to the incident beam and shifted to the lower level. Then, the beam propagated through the compressor in the backward direction was again reflected from gratings (*2*) and (*1*), passed under mirror (*4*), and fell on the system of output mirrors (*5–8*).

Mirror (*5*) with a reflection coefficient of 99% and a homogeneous transmission spectrum in the entire 860–960-nm region served for coupling out the radiation from the compressor for diagnostics of the energy, spatial, and spectral characteristics of the compressed pulse. To measure the pulse duration, a movable mirror (*10*) with an aperture of 12×12 mm in size sent a part of the beam to a single-pulse autocorrelator. About 7% of radiation incident on the first grating was zero-order diffracted (mirror reflected) (see Fig. 1). This radiation, after reflection from mirror (*5*), was used as a reference of the small grating position in the system of compressor alignment and diagnostics.

The calculated angle of beam incidence on the first grating of the compressor was 43.1° (Littrow angle plus 10°). According to calculations, at the normal distance between the gratings of 133.75 cm, the compressor compressed the chirped pulses from the duration $\tau = 0.5$ ns to 37 fs. All the optical elements of the compressor, including auxiliary optics, were remotely controlled by a computer. Step motors equipped with reducers ensured the rotation and replacement accuracy of a few angular seconds and micrometers, respectively.

3. Compressor alignment system

The accuracy required for alignment of the angular positions of the optical units of a compressor can be estimated by comparing the output beam divergence, which is caused by the deviation of angles from the calculated values, with the diffraction limit. For a laser beam with the central wavelength 0.91 μm and a diameter of 11 cm, the diffraction limit divergence is $\sim 2''$. To achieve the same divergence of a broadband radiation with wavelengths within the region of 0.86–0.96 μm in a double-pass compressor based on two gratings with a density of 1200 lines mm^{-1}, it is necessary to rotate the second grating around the vertical axis by an angle of $\sim 14''$. The accuracy for the signal radiation with a larger beam diameters and a wider spectrum must be higher.

The optical scheme of alignment of a two-grating compressor is shown in Fig. 2. The beam of an alignment laser with a wavelength of 0.91 μm propagated along the signal beam path and coincided with this beam in direction and transverse size. Mirror (*1*) sent this beam to the compressor. On the way, the beam passed through an optical glass wedge (*6*) with an angle of 10′. About 1% of the power was reflected to a triple mirror (TM) – corner reflector made of three aluminum-coated mirrors with angular positioners for adjustment of 90° angles between the mirrors with a second accuracy. The alignment laser beam reflected from the triple mirror propagated through the wedge, was focused by a lens system onto a CCD camera, and served as a reference for the direction of the signal beam sent to the compressor. The He–Ne laser beam with a wavelength of 0.63 μm passed through a beam expanding telescope (ET), which increased the beam diameter to 5 cm, and was superposed with the signal beam by mirrors (*2*) and (*3*). For coincidence of the focal planes of the 0.63- and 0.91-μm radiations on the CCD camera, the He–Ne laser beam was converged using a slight misalignment of the

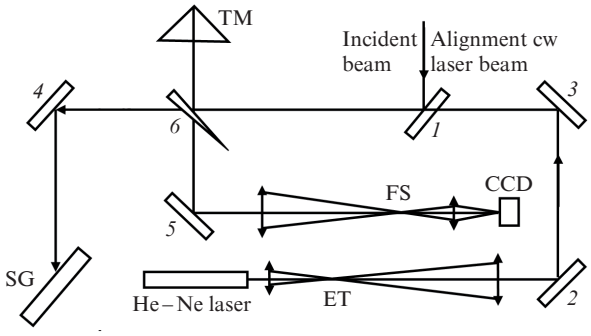

Figure 2. Compressor alignment system (view from above): (*1–5*) deflecting mirrors; (*6*) wedge glass plate; (SG) small grating of the compressor; (ET) expanding telescope; (FS) focusing system; (TM) triple mirror.

expanding telescope base. In this case, the positions of the reference beams with these wavelengths did not coincide. We made necessary calculations of corrections for the wedge plate dispersion, which were taken into account when aligning the compressor.

4. Design of the grating unit of a subpetawatt compressor

The decisive role in the precise alignment of the compressor was played by the specially designed mechanical mounts for diffraction gratings. This design allowed manual and remote alignment of gratings over the three rotational degrees of freedom with a second accuracy.

The principal scheme of the small grating unit is shown in Fig. 3a. In the bottom of the unit, we placed a rotator, which allowed manual rotation of the grating by 360° around the vertical axis with turned-off lock screws and, with fixed screws, allowed rotation with a step motor within 12° with an accuracy of 6″ without reducer and with an accuracy of a portion of an angular second with the use of a reducer.

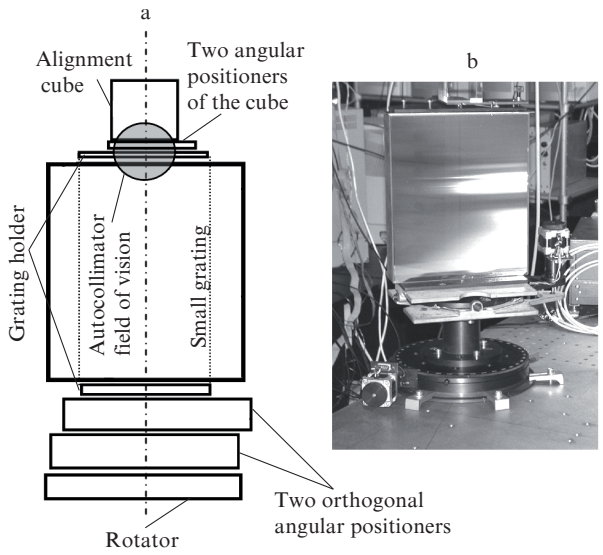

Figure 3. Principal scheme of the compressor grating unit (a) and its photograph (b).

The holder with the small grating was placed on an optical table, which was fixed on a rotary platform (Fig. 3b). To control the grating tip and align the groove direction, the table was equipped with two positioners, which allowed one to rotate the table with respect to the horizontal axes (parallel and perpendicular to the grating surface) within several degrees with a second accuracy.

At the top of the grating holder, we placed an additional table with an alignment cube made of K-8 optical glass. The opposite polished faces of the cube were pairwise parallel with a second accuracy. Two independent angular positioners of the table made it possible to align the cube with respect to two orthogonal horizontal axes. In our scheme, the cube was placed maximally close to the grating, so that one could simultaneously observe them in an autocollimator (the beam diameter of the used AKT-15 autocollimator was ~50 mm). The autocollimator field of vision is indicated by a circle in Fig. 3a.

The large grating unit of the subpetawatt compressor was designed similarly to the scheme described above. The differences consisted in the absence of the alignment cube and in the presence an additional longitudinal translator for controlling the compressor base. In subsequent modifications, the grating unit was additionally supplied with a special platform, which allowed us to control and align the vertical rotation axes of all the compressor gratings parallel to each other.

The vertical roof mirror (see Fig. 1) was also mounted on a rotary device and had one more angular positioner which made it possible to rotate it as a whole around the horizontal axis perpendicular to the line of intersection of the surfaces of mirrors.

5. Grating unit alignment method

The alignment of the grating unit consisted in the precise positioning of the grating surface and the groove direction parallel to the vertical rotation axis. The alignment was performed in several successive stages using an autocollimator and an alignment cube. For convenience of subsequent alignment, the cube was positioned so that the image of the autocollimation reticle reflected from one of the cube faces almost coincided with the reticle image from the grating surface.

The autocollimator axis was aligned perpendicular to the rotation axis of the grating unit rotator similarly to the procedure of determination of the non-parallelism of the rotation axes of the alidade and the table with the limb of the goniometer [31]. First, the autocollimator was adjusted perpendicular to one of the cube faces in position I (Fig. 4), after which the cube together with the grating was rotated by 180° into position II. This lead to a vertical shift of the image of the autocollimation reticle in the autocollimator. Then, the autocollimator was rotated to position III, by the angle corresponding to the half of the angle of the shift of the autocollimation reticle image, and the cube was also rotated in the opposite direction by the same half-angle. The iteration procedure – rotation of the grating unit by 180° and rotation of the autocollimator and the cube by half-angles – is convergent. As a result, the autocollimator axis is aligned strictly perpendicular to the rotation axis of the grating unit, as well as to the cube faces used for alignment.

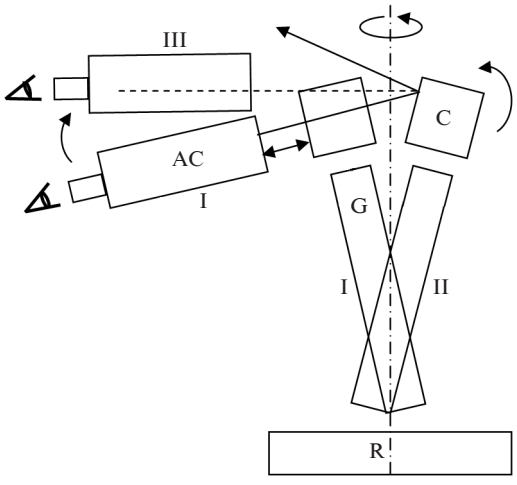

Figure 4. Scheme of alignment of the autocollimator axis perpendicular to the rotation axis of the grating unit: (AC) autocorrelator; (C) cube; (G) grating; and (R) rotator.

At the next step of alignment, the autocollimator remained in this aligned position. The grating unit was rotated by 90°. The third face of the cube was aligned normally to the collimator beam using the corresponding angular adjustment screws. Since the faces of the alignment cube are pairwise parallel, the fourth face of the cube, when rotated toward the collimator, must also be precisely perpendicular to its axis. However, this turned out to be wrong for our grating unit. We explained this fact by technical reasons, namely, by inequality of the sizes of the rotator bearing balls, non-identical tightening of fixing bolts, nonuniform load to the bearing (the grating with the holder weighed several kilograms).

Since the cube was made of transparent glass, the reticle images were also seen in the intermediate positions of the cube with respect to the autocollimator axis (Fig. 5a). Thus, rotating the cube, one can plot a graph of the rotator axis drift in the process of rotation. In the blind zones, in which the autocollimation reticle image is not seen, one can observe the cube rotation from another angle using an additional mirror. Figure 5b shows a typical shape of such a plot. Usually, the axis drifts are very small (a few angular seconds) and are very difficult to avoid. However, for subsequent alignment of the grating, it is important to choose a rotation range within 12°–15° with the minimum drift of the axis. This range is denoted in Fig. 5b as working region. The rotator was adjusted so that, within the found working region, it was possible to remotely rotate the grating using the step motor from the position corresponding to the Littrow angle for the beam incident on the compressor to the working angle of beam incidence on the grating.

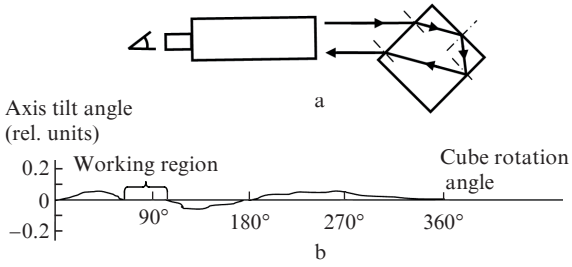

Figure 5. Reflection of the collimator beam in the intermediate positions of the alignment cube (a) and typical dependence of the axis drift on the cube rotation angle (b). The rotation axis is perpendicular to the plane of the figure.

The next step consisted in the alignment of the grating itself with respect to the rotation axis. Making sure that the cube face is parallel to the rotation axis, the autocollimator was positioned so that it was possible to observe the reticle images simultaneously from the cube and the grating. Then, the reticle image from the cube was matched with the crosshair of the autocollimator, and the grating was rotated to this position using the positioners of the grating tip and rotation (this procedure disturbed the cube alignment). Note that if one of the cube faces is beforehand positioned strictly parallel to the working surface of the grating, then one can use the corresponding angular positioners of the grating holder from the beginning of the above-described alignment.

To align the grating grooves parallel to the rotation axis of the rotator, the autocollimator axis was positioned normally to the working surface of the grating and the reticle image was matched with the crosshair. Then, the grating was rotated to an angle at which the first Littrow reflection of the autocollimator beam was observed (Fig. 6). Rotating the autocollimator tube with respect to its optical axis, we minimised the thickness of the image of the central horizontal line of the autocollimation reticle. The line image was clear, though spectrally coloured, and allowed us to perform measurement with an accuracy to 3″, which corresponded to the reticle line thickness. The vertical shift of the colour line with respect to the crosshair is caused by the tilt of the grating grooves. Rotating the grating around the horizontal axis that is perpendicular to the working surface using the corresponding adjusting screw, we matched the colour images of the reticle line and the crosshair, which meant that the grating grooves are aligned parallel to the grating vertical rotation axis. It should be noted that the numerical processing of the autocollimation reticle image can easily ensure a subsecond accuracy of autocollimation measurements.

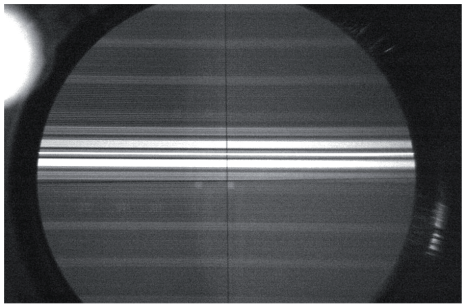

Figure 6. Pattern observed in the autocollimator in the process of alignment of grooves when the grating is rotated to the Littrow angle.

6. Adjustment of the working positions of compressor units

The next step in assembling of the compressor is the alignment of the incident beam direction perpendicular to the rotation axis of the small grating. To do this, we rotated the grating surface normally to the incident alignment beam (see Figs 1 and 2). The beam reflected by the grating exited the compressor, fell onto an optical wedge, was partially reflected to the recording part of the compressor adjustment system, and was focused on the matrix of the CCD camera. Matching of this image with the reference one using transport mirror (*4*), we obtain that the signal beam incident on the grating is perpendicular to the rotation axis and, hence, to the grooves.

When the small grating was rotated to the Littrow angle for the alignment beam, the CCD camera recorded the far-field image of this beam spread into the spectrum: a long brightness-modulated horizontal line, which intersected the reference point. The matter is that the alignment fibre laser emitted cw radiation at a wavelength of 910 nm with a bandwidth of several nanometers. The measurements of the alignment laser spectrum showed four–five characteristic peaks of different intensities. These peaks were well identified, and each of them was attributed to a definite measured wavelength. Thus, knowing the grating groove density and the wavelength, we were able to determine the exact angle of beam incidence on the small grating.

To adjust the large grating of the compressor, we placed the small grating at the Littrow angle to the 910-nm incident beam (Fig. 7). Then, a He–Ne laser beam with a wavelength of 633 nm was directed along the same direction. This beam was reflected in the first diffraction order at an angle of 12.3° with respect to the normal to the small grating. It is known that the Littrow angle for 633-nm radiation for a grating with the groove density of 1200 lines mm^{-1} is 22.3°. Therefore, the adjustment of the large grating into the position at which the He–Ne laser beam is reflected precisely backward corresponds to the working position of the grating. The large grating was adjusted using two angular positioners up to the matching of the images of the reference He–Ne laser beam with the He–Ne laser beam passed through the compressor in the diagnostics system. In this case, we can make sure that the grooves of the large grating are perpendicular to the incident beam and, hence, the plane of the large grating is perpendicular to the plane of the beam propagation in the compressor. Moreover, taking into account the known wavelength of alignment beams, it is possible to calculate the grating rotation angles with a second accuracy. If needed, it is possible to introduce corrections taking into account the difference between the alignment beam wavelength and the central wavelength of the signal radiation of the system.

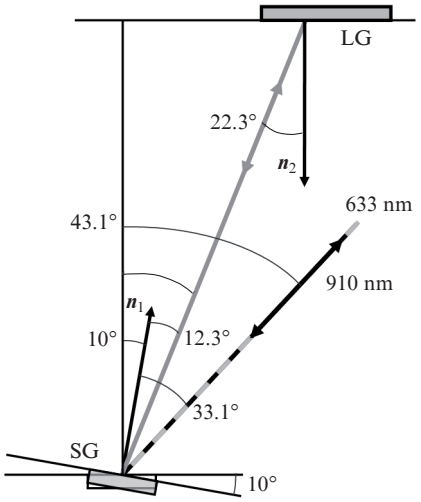

Figure 7. Scheme of alignment of the large diffraction grating of the compressor: (SG) small grating; (LG) large grating.

By the step motor of the PC-controlled rotator, the small grating was rotated by 10° (into the working position). To do this, we used the previously determined dependences of the grating rotation angle on the number of steps of the step motor.

The vertical roof mirror was placed into the working position by using the apertured alignment beam with a wavelength of 910 nm so that after reflection from the reflector it propagated backward in the lower level strictly under the incident beam.

The criteria of the completed alignment of the compressor were the output radiation parameters: the minimum pulse duration, uniform duration over the transverse beam coordinate, good beam collimation, and the absence of angular dispersion.

The output pulse duration was minimised by changing the compressor base due to a parallel shift of the large grating. The translator was equipped with a step motor and was remotely controlled. The shift corresponding to one step of the step motor was 2.5 μm. The compressor output pulse duration was measured by a single-shot autocorrelator based on noncollinear second harmonic generation.

The residual angular dispersion was controlled with a spectrograph [32, 33], which measured the angular dependence of the spectrum (spectrum diagram) of radiation at the compressor exit. To measure the angular dispersion in two orthogonal planes, the spectrograph was successively rotated by 90° with respect to the normal to the input slit. The residual angular dispersion, if existed, was eliminated by alignment of the large grating and the corner reflector.

7. Method of measurement of the difference in the groove densities of gratings

It is known that, even at perfectly aligned parallel planes and grooves of the compressor gratings, the output radiation may exhibit uncompensated residual angular dispersion caused by different groove densities of the used gratings [6, 22, 23].

To measure the difference in the groove densities of diffraction gratings, we placed the two studied gratings close to each other so that it was possible to simultaneously observe their working surfaces in the autocollimator. First, using the autocollimator positioned normally to the gratings, the surfaces are aligned parallel to each other by two angular positioners. Then, seeing the gratings in the autocollimator at the Littrow angle, the grooves are aligned mutually parallel using the corresponding adjustment screws. In this process, one of the gratings is rotated to the coincidence of two colour horizontal lines (see Fig. 6) – spectrally spread images of the autocollimation reticle. As a result of alignment, the working surfaces and grooves of the two studied gratings became parallel to each other with an accuracy of $\sim 3''$.

After this, a He–Ne laser beam is sent to the gratings at an angle α. In the case of different groove densities of the gratings N_1 and N_2, the reflection angles Θ_1 and Θ_2 are different. From the grating formula

$$\sin\alpha + \sin\Theta_i = m\lambda N_i$$

in the case of close Θ_1 and Θ_2 angles, we obtain the following expression for the difference in the groove densities:

$$\Delta N = \Delta\Theta\cos\Theta/m\lambda,$$

where λ is the radiation wavelength, $i = 1, 2$ is the grating number, and m is the diffraction order.

At the measurement accuracy $\Delta\Theta_{\min} = 3''$ achieved when using an autocollimator with visual detection, for the diffraction angle $\Theta = 60°$ and $\lambda = 633$ nm, we obtain $\Delta N_{\min} = 0.01$ and 0.005 lines mm^{-1} for the first and second diffraction orders, respectively. The measurement accuracy can be improved by more than an order of magnitude by using grazing reflection angles and digital recording of radiation reflected from the gratings.

8. Conclusions

An original method of adjustment of a chirped-pulse compressor of high-power femtosecond CPA lasers is described in detail. The method allows one to align diffraction gratings with a second accuracy in three degrees of freedom, including

alignment of the direction of grooves, as well as to adjust the angles of beam incidence on the gratings. As a result of the fulfilled adjustment of the stretcher and compressor of a PEARL laser system, laser pulses with a peak power of 0.56 PW at a duration of 43 fs are obtained.

A simple method for measuring the difference in the groove densities of gratings with an accuracy better than 0.005 lines mm^{-1} is proposed and tested. Knowledge of this value is necessary for calculating and cancelling the residual angular dispersion of the compressor. The measurements of the difference in the groove densities are especially important in the case when one of the gratings must be replaced for a new grating of another batch.

The methods proposed in this work can be used for adjustment of existing and being developed petawatt and multi-petawatt CPA systems, including the systems with tiled (mosaic) gratings.

References

1. Strickland D., Mourou G. *Opt. Commun*., **56**, 219 (1985).
2. Treacy E.B. *IEEE J. Quantum Electron*., **QE-5**, 454 (1969).
3. Martinez O.E. *IEEE J. Quantum Electron*., **QE-23**, 59 (1987).
4. Osvay K., Ross I.N. *Opt. Commun*., **105**, 271 (1994).
5. Fiorini C., Sauteret C., Rouyer C., Blanchot N., Seznec S., Migus A. *IEEE J. Quantum Electron*., **30**, 1662 (1994).
6. Zhang T., Yonemura M., Kato Y. *Opt. Commun*., **145**, 367 (1998).
7. Pretzler G., Kasper A., Witte K.J. *Appl. Phys. B*, **70**, 1 (2000).
8. Osvay K., Kovács A.P., Heiner Z., Kurdi G., Klebniczki J., Csatári M. *IEEE J. Sel. Top. Quantum Electron*., **10**, 213 (2004).
9. Kovács A.P., Osvay K., Kurdi G., Görbe M., Klebniczki J., Bor Z. *Appl. Phys. B*, **80**, 165 (2005).
10. Osvay K., Kovács A.P., Kurdi G., Heiner Z., Divall M., Klebniczki J., Ferincz I.E. *Opt. Commun*., **248**, 201 (2005).
11. Ross I.N., Trentelman M., Danson C.N. *Appl. Opt*., **36**, 9348 (1997).
12. Miesak E., Negres R. *Appl. Opt*., **37**, 8146 (1998).
13. Collier J.L., Hernandez-Gomez C., Hawkes S.J., Smith J., Winstone T.B., et al. in *Rutherford Appleton Laboratory. Central Laser Facility Annual Report 2002/2003* (2003) p. 168.
14. Liu F., Liu X., Wang Z., Ma J., Zhang L., Wang J., Wang S., Lin X., Li Y., Chen L., Wei Z., Zhang J. *Appl. Phys. B*, **101**, 587 (2010).
15. Guardalben M.J. *Appl. Opt*., **47**, 4959 (2008).
16. Varjú K., Kovács A.P., Kurdi G.K.O. *Appl. Phys. B*, **74**, S259 (2002).
17. Sacks Z., Mourou G., Danielius R. *Opt. Lett*., **26**, 462 (2001).
18. Chvykov V., Yanovsky V. *Proc. CLEO/IQEC* (Baltimore, 2009).
19. Ruiz-de-la-Cruz A., Rangel-Rojoand R. *Revista Mexicana de Fisica*, **51**, 488 (2005).
20. Lozhkarev V.V., Freidman G.I., Ginzburg V.N., Katin E.V., Khazanov E.A., Kirsanov A.V., Luchinin G.A., Mal'shakov A.N., Martyanov M.A., Palashov O.V., Poteomkin A.K., Sergeev A.M., Shaykin A.A., Yakovlev I.V. Preprint IAP No.720 (N. Novgorod, 2006).
21. Lozhkarev V.V., Freidman G.I., Ginzburg V.N., Katin E.V., Khazanov E.A., Kirsanov A.V., Luchinin G.A., Mal'shakov A.N., Martyanov M.A., Palashov O.V., Poteomkin A.K., Sergeev A.M., Shaykin A.A., Yakovlev I.V. *Laser Phys. Lett.*, **4**, 421 (2007).
22. Rushford M.C., Britten J.A., Barty C.P.J., Jitsuno T., Kondo K., Miyanaga N., Tanaka K.A., Kodama R., Xu G. *Opt. Lett*., **33**, 1902 (2008).
23. Hornung M., Bödefeld R., Kessler A., Hein J., Kaluza M.C. *Opt. Lett*., **35**, 2073 (2010).
24. Kessler T.J., Bunkenburg J., Huang H., Kozlov A., Meyerhofer D.D. O*pt. Lett*., **29**, 635 (2004).
25. Hornung M., Bödefeld R., Siebold M., Schnepp M., Hein J., Sauerbrey R., Kaluza M.C. *Appl. Opt*., **46**, 7432 (2007).
26. Freidman G., Andreev N., Ginzburg V., Katin E., Khazanov E., Lozhkarev V., et al. *Proc. SPIE Int. Soc. Opt. Eng*., **4630**, 135 (2002).
27. Lozhkarev V.V., Freidman G.I., Ginzburg V.N., Khazanov E.A., Palashov O.V., et al. *Laser Phys*., **15**, 1319 (2005).
28. Lozhkarev V.V., Garanin S.G., Gerke R.R., Ginzburg V.N., Katin E.V., Kirsanov A.V., et al. *Pis'ma Zh. Eksp. Teor. Fiz*., **82**, 196 (2005) [*JETP Lett*., **82**, 178 (2005)].
29. Lozhkarev V.V., Freidman G.I., Ginzburg V.N., Katin E.V., Khazanov E.A., Kirsanov A.V., Luchinin G.A., Mal'shakov A.N., Martyanov M.A., Palashov O.V., Poteomkin A.K., Sergeev A.M., Shaykin A.A., Yakovlev I.V., et al. *Opt. Express*, **14**, 446 (2006).
30. Freidman G.I., Yakovlev I.V. *Kvantovaya Elektron*., **37** (2), 147 (2007) [*Quantum Electron*., **37** (2), 147 (2007)].
31. State standard of the USSR. Goniometry. Metody i sredstva poverki (Goniometers. Methods and techniques) No. 8.266-77 (Moscow, 1978).
32. Freidman G., Andreev N., Bespalov V., Bredikhin V., Ginzburg V., Katin E., Korytin A., Khazanov E., Lozhkarev V., Palashov O., Sergeev A., Yakovlev I., et al. *Proc. CLEO* (Long Beach, CA, 2002).
33. Freidman G., Andreev N., Bespalov V., Bredikhin V., Ginzburg V., Katin E., Khazanov E., Korytin A., Lozhkarev V., Palashov O., et al. *Proc. SPIE Int. Soc. Opt. Eng*., **4972**, 90 (2003).